Biochimica et Biophysica Acta 1822 (2012) 546–549

Contents lists available at SciVerse ScienceDirect

Biochimica et Biophysica Acta

journal homepage: www.elsevier.com/locate/bbadis

Reduction in neuronal L-type calcium channel activity in a double knock-in mouse model of Alzheimer's disease

Olivier Thibault [a,*], Tristano Pancani [a], Philip W. Landfield [a], Christopher M. Norris [a,b,**]

[a] Department of Molecular and Biomedical Pharmacology, University of Kentucky College of Medicine, Lexington, KY 40536, USA
[b] Sanders-Brown Center on Aging, University of Kentucky College of Medicine, Lexington, KY 40536, USA

ARTICLE INFO

Article history:
Received 31 October 2011
Received in revised form 20 December 2011
Accepted 4 January 2012
Available online 10 January 2012

Keywords:
Calcium dyshomeostasis
Alzheimer's disease
Hippocampus
Cognitive impairment

ABSTRACT

Increased function of neuronal L-type voltage-sensitive Ca^{2+} channels (L-VSCCs) is strongly linked to impaired memory and altered hippocampal synaptic plasticity in aged rats. However, no studies have directly assessed L-VSCC function in any of the common mouse models of Alzheimer's disease where neurologic deficits are typically more robust. Here, we used cell-attached patch-clamp recording techniques to measure L-VSCC activity in CA1 pyramidal neurons of partially dissociated hippocampal "zipper" slices prepared from 14-month-old wild-type mice and memory-impaired APP/PS1 double knock-in mice. Surprisingly, the functional channel density of L-VSCCs was significantly reduced in the APP/PS1 group. No differences in voltage dependency and unitary conductance of L-VSCCs were observed. The results suggest that mechanisms for Ca^{2+} dysregulation can differ substantially between animal models of normal aging and models of pathological aging.

1. Introduction

Central to the Ca^{2+} hypothesis of brain aging is the concept of "Ca^{2+}-as-mediator" of neurologic dysfunction associated with age and age-related diseases, such as Alzheimer's disease (AD) [1–7]. Extensive support for the Ca^{2+} hypothesis comes from studies on both normal and pathologic aging using a variety of animal models and diverse experimental approaches. However, whether some Ca^{2+} signaling mechanisms contribute primarily to normal aging deficits or are more relevant for disease symptoms remains largely unknown. Elevated activity of L-type voltage sensitive Ca^{2+} channels (L-VSCCs) in hippocampal neurons [8] has provided one of the most robust links to altered membrane excitability, impaired synaptic function, and cognitive decline in animal models of normal aging (for review see [6]). In contrast, no studies have measured neuronal L-VSCC currents in any of the common mouse models of AD. Here, we used the partially-dissociated hippocampal "zipper" slice preparation and cell-attached patch-clamp to assess L-VSCC properties in CA1 pyramidal neurons of mid-age (14–15 months) wild-type mice and memory-deficient AD (*i.e.* APP/PS1) mice. The results revealed a marked reduction in L-VSCC activity in the APP/PS1 group, suggesting that Ca^{2+} dysregulation may be independent of L-VSCC function in some transgenic mouse models of AD.

2. Materials and methods

2.1. Transgenic mice

Homozygous male $APP^{NLh/NLh}$ X $PS\text{-}1^{P264L/P264L}$ mice, maintained on a CD-1/129 background, were used at 14-months-of-age. These mice deposit humanized Aβ by 6 months, and exhibit extensive plaque pathology by 14 months [9]. Wild-type mice were initially obtained from matings between APP/PS1 heterozygotes, and then maintained as a separate line. Mice were maintained on a 12 h:12 h light–dark cycle and had *ad libitum* access to rodent chow. All procedures were compliant with the guidelines of the University of Kentucky institutional animal use committee and the American Association for Accreditation of Laboratory Animal Care.

2.2. One-way active avoidance

On each trial, mice were placed in the dark compartment of a standard two compartment active avoidance chamber. After a seven second grace period, a 25 s 0.8 mA shock was delivered through the floor of the dark compartment and escape time to the light compartment was recorded. Mice were placed in a temporary holding cage for 60 s between trials. An escape time ≤7 s was considered to be an "avoidance". The percent of successful avoidances for each mouse was averaged across four trials on each day (four days total), normalized to day 1 performance levels for each mouse, and compared

* Correspondence to: O. Thibault, 800 Rose St, MS320 Chandler Medical Center, Univ Kentucky College of Medicine, Lexington, KY 40536, USA. Tel.: +1 859 323 4863; fax: +1 859 323 1981.
** Correspondence to: C.M. Norris, 800 South Limestone St., 131 Sanders-Brown Building, Univ Kentucky College of Medicine, Lexington, KY 40536, USA. Tel.: +1 859 257 1412x249; fax: +1 859 323 2866.
E-mail addresses: othibau@uky.edu (O. Thibault), cnorr2@uky.edu (C.M. Norris).

0925-4439/$ – see front matter © 2012 Elsevier B.V. All rights reserved.
doi:10.1016/j.bbadis.2012.01.004

across training days and genotype using repeated measures ANOVA ($p<0.05$).

2.3. Cell-attached patch clamp recording in hippocampal zipper slices

Preparation of partially dissociated "zipper" slices from mice was carried out as described by earlier studies on adult guinea pigs [10] and aged rats [8,11,12]. Mice were decapitated after CO_2 asphyxiation, and brains placed briefly in ice-cold oxygenated (95%O2/5%CO2) artificial cerebral spinal fluid (ACSF) containing (in mM): 114 NaCl, 2.5 KCl, 2 $MgCl_2$, 30 $NaHCO_3$, 10 Glucose, and 0.1 $CaCl_2$ (pH 7.4). Coronal slices (300 μm) were made in ice-cold ACSF using a Vibratome® as described [13] and transferred to prewarmed (32 °C), oxygenated ACSF containing 2 mM $CaCl_2$ and 0.7 mg/ml pronase for 30 min. Slices were washed twice in ACSF followed by an additional 15 min in ACSF containing 0.5 mg/ml thermolysin. After two more washes in ACSF, slices were bathed for 1–4 h in enzyme-free, ACSF with 2 mM $CaCl_2$. To expose CA1 pyramidal neurons for patch clamp recordings, slices were nicked at CA1 *stratum pyramidale* near the border of the subiculum using a scalpel blade, then transferred to a 2 mL analyzing cup containing ~1 mL of Ca^{2+}-free ACSF and gently shaken by hand until clear dissociation was observed along CA1 stratum pyramidale.

Glass recording pipettes (5.6 ± 0.14 MΩ) were coated with Sylgard® and fire-polished immediately before use. External recording solution contained (in mM): 140 K^+-gluconate, 3 $MgCl_2$, 10 glucose, 10 EGTA, and 10 HEPES, pH = 7.35, osmolarity = 300 mOsm. Pipette solution contained (in mM): 20 $BaCl_2$, 90 choline Cl, 10 TEA Cl, and 10 HEPES, 0.0005 Bay K 8644 (L-VSCC activator), pH = 7.35, osmolarity = 290 mOsm. Junction potentials were nulled in the bath and tip resistances determined prior to obtaining a giga-ohm seal from cleanly exposed CA1 neurons. *I/V* curves were constructed by successively stepping (150 ms) the membrane voltage (V_m) in 10 mV increments from holding (−70 mV) to +40 mV. Current amplitudes (*i*) of clearly resolvable L-VSCC openings were also measured at different V_m levels (*i.e.* −70 to +10 mV; one sec duration steps) to assess slope conductance (in pS) of L-VSCCs. The V_m was then stepped from −70 to the maximal activating voltage (0 or +10 mV) a total of 90 times (10 s interstep interval) to find the maximal instantaneous current (I_{max}, see below) and to generate an average ensemble current for each patch. Currents were leak-subtracted off-line using hyperpolarizing pulses, identical in duration and opposite in polarity. Average current density (pA/μm^2) was derived by dividing the average ensemble current by the patch area ($a = 12.6(1/R + 0.018)$, where 'a' is the patch area and 'R' is the pipette resistance [14]. The method of maximum instantaneous openings was used to estimate the total number of channels in a patch (N) by dividing I_{max} by the single channel average amplitude (*i.e.* $N = I_{max}/i$) as described [8,15]. This value was then divided by patch area to estimate channel density (N/μm^2). All recordings were obtained at room temperature, filtered at 2 kHz, and digitized at 5 kHz using an Axoclamp 1D patch-clamp amplifier and Clampex software. All VSCC properties were measured offline using Clampfit software and compared between genotypes using unpaired, two-tailed Student's T tests ($p<0.05$).

3. Results

3.1. 2xTg mice show impairments on a one-way active avoidance task

At 14 months, 10 male WT and 7 male 2xTg mice were trained across four days on a standard one-way active avoidance task (4 trials/day, see Materials and methods). Optimal performance on this task requires a functionally intact hippocampus [16]. As shown in Fig. 1, the percent of trials in which mice exhibited a successful avoidance was calculated on each day and normalized to day 1 performance. WT and 2xTg animals showed nearly identical performance levels on day 1. While both groups exhibited a higher percentage of avoidances with each successive training day ($p<0.001$), 2xTg mice were generally outperformed by their WT counterparts ($p<0.05$). Thus, like many other AD transgenic models, the APP/PS1 double knock-in mice used here exhibit a measurable cognitive deficit.

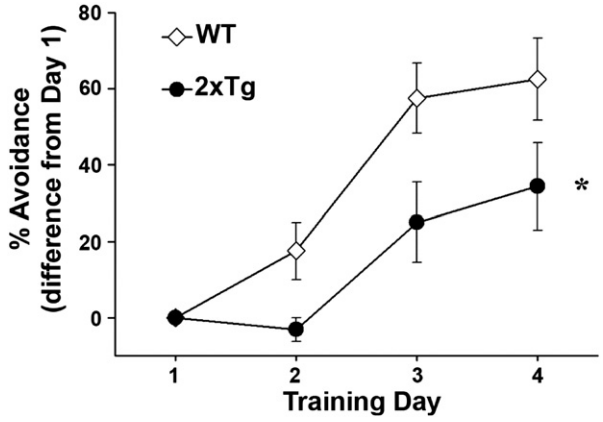

Fig. 1. 2xTg mice show deficits on a standard one-way active avoidance task. Line graph shows mean ± SEM percent avoidances on each training day (normalized to Day 1 performance) for WT and 2xTg mice. * indicates significantly poorer performance in 2xTg mice across all training days ($p<0.05$, repeated measures ANOVA).

3.2. Neuronal L-VSCC currents are reduced in 2xTg mice

Hippocampal zipper slices were prepared from 13 of the behaviorally characterized mice shown in Fig. 1 (WT, $n=7$; Tg, $n=6$). On-cell patch clamp analysis of L-VSCC currents from CA1 pyramidal neurons were made as described previously by our labs [8,11,12]. Thirty-five patches were recorded across both groups (WT, $n=19$; 2xTg, $n=16$). No differences in pipette tip resistance, seal resistance, or the maximal activating voltage (*i.e.* the membrane potential associated with maximal L-VSCC activity) were observed (Table 1). For all L-VSCC properties measured, values were averaged across patches within each mouse and used for statistical comparisons (*i.e.* $n=$ # of mice/group). Representative L-VSCC ensemble currents during step depolarizations from −70 to +10 mV in patches taken from a WT and 2xTg mouse are shown in Fig. 2A, and the average ± SEM ensemble peak current density (pA/μm^2) is shown in Fig. 2B. The results revealed a significant reduction in maximal L-VSCC current density in the 2xTg group ($p<0.05$). No change in L-VSCC voltage dependency was observed. Analysis of single channel properties indicated similar unitary L-VSCC current (*i*) amplitudes across V_m levels for both groups (Fig. 2C) and no differences in slope conductance were found. Using the method of maximal instantaneous openings to estimate the total number of channels (N) per patch [8,15], we observed a greater than two-fold reduction in L-VSCC channel density (N/μm^2) for the 2xTg group. These results suggest that lower L-VSCC activity in 2xTg mice is largely due to a reduction in the number of functional channels in the plasma membrane.

Table 1
Electrode and cell parameter values expressed as mean + SEM. No group differences were observed.

	Number of patches	Number of mice	Electrode resistance (MΩ)	Seal resistance (GΩ)	Maximal activation voltage (mV)
WT	19	7	5.71 + 0.23	22 + 2.57	6.67 + 1.98
2xTg	16	6	5.58 + 0.16	28.67 + 4.84	6.88 + 1.5

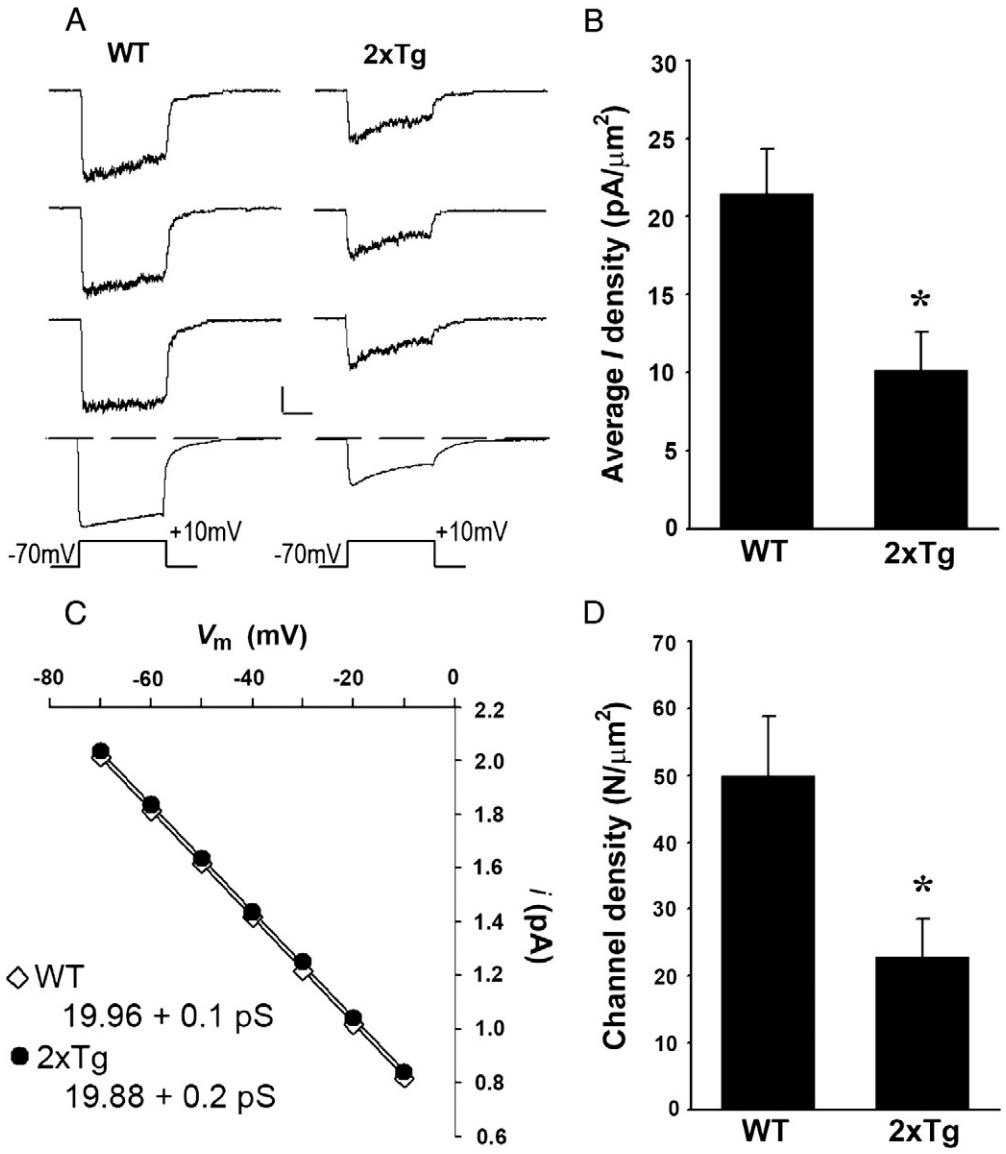

Fig. 2. CA1 neuronal L-VSCC activity is reduced in 2xTg mice. A, Representative L-VSCC current traces (top 3 waveforms), and the average ensemble current (lowest trace) generated from 90-step depolarizations in multichannel cell-attached patches from WT and 2xTg mice. Maximal L-VSCC activity was elicited by stepping the patch membrane from −70 to +10 mV for 150 ms. Scale bars: 20 pA/50 ms. B, mean ± SEM peak ensemble current density (pA/μm^2) in each genotype group. C, mean ± SEM unitary L-VSCC current amplitudes (*i* in pA) measured at different membrane potentials (V_m in mV). No genotype differences in slope conductance were observed. D, mean ± SEM functional channel density in cell-attached patches from each genotype. *significant reduction relative to WT mice ($p<0.05$, two-tailed unpaired T tests).

4. Discussion

L-VSCC activity is potentiated during aging [8,11] and plays a significant role in age-related alterations in synaptic function [17,18], membrane excitability [19], and cognition [20,21]. There are several lines of evidence to suggest that L-VSCCs may also contribute to the pathophysiology of AD. Postmortem AD brain is associated with increased radiolabel binding to L-VSCCs [22], and L-VSCC activity in cell cultures is elevated following delivery of pathogenic Aβ peptides [23–30]. However, the present study is the first to directly assess neuronal L-VSCC activity in a mouse model of AD. The mid-aged double knock-in Tg mice used here exhibit high brain tissue levels of both soluble and insoluble Aβ [9], as well as significant cognitive impairment (Fig. 1). It was therefore somewhat surprising to observe a reduction, rather than an increase, in neuronal L-VSCC currents in Tg mice (Fig. 2).

The mechanistic basis for reduced L-VSCC activity is not presently known, but it seems unlikely that 2xTg mice simply lack sensitivity to age-dependent mechanisms implicated in gain-of-function. The cyclic AMP dependent protein kinase (PKA) and the protein phosphatase calcineurin have each been proposed to augment L-VSCC activity during aging [11,31,32]. While evidence for impaired activation of PKA and/or PKA dependent processes has been reported in AD mice and/or cell cultures treated with Aβ [33,34], calcineurin activity and signaling are upregulated in the same or similar models [35–38]. Moreover, previous work by Stutzmann and colleagues on single and triple Tg models of AD revealed an age-dependent increase in the post-burst afterhyperpolarization, a Ca^{2+} dependent event requiring L-VSCC activation [39].

The findings of the present study may be more closely associated with functional changes inherent to the PS1 mutation. PS1 is a resident protein of the endoplasmic reticulum (ER) and is functionally coupled to key ER Ca^{2+} release channels (*e.g.* IP3 receptors and ryanodine receptors) that are also juxtaposed to L-VSCCs. Indeed, it is well established that L-VSCCs operate in series with ER channels to mediate Ca^{2+}-induced Ca^{2+} release (CICR) in neurons [40]. During aging, in which Ca^{2+} dysregulation is relatively mild, elevations in L-VSCC activity are clearly able to co-exist with elevations in CICR

[41–43]. However, abnormal gating properties and expression levels of ER Ca^{2+} channels associated with PS1 mutations [44] may drive Ca^{2+} levels high enough to ultimately deliver negative feedback onto L-VSCCs, as shown previously for NMDA receptors [45]. Clearly, it will be important to conduct extensive investigations on singly transgenic mice (mice that express the human APP mutation, but lack mutant PS1, and *vice versa*) at multiple age points to determine the relative contributions of PS1 and aging to L-VSCC regulation. Further work on single knock-in mice may also offer increased relevancy to AD, since humans rarely if ever co-express APP and PS1 mutations.

In summary, the present study revealed a significant reduction in neuronal L-VSCC activity in a double knock-in mouse model of AD. These results were unexpected based on extensive evidence of enhanced L-VSCC activity in animal models of aging and cell culture models of amyloid toxicity. Our findings, together with previous work, suggest that the directional regulation of L-VSCC activity during AD depends on a complex interaction between aging, circulating Aβ levels, the presence of PS1 variants, and the degree of existing Ca^{2+} dysregulation, among other factors. Clearly, additional work on other Tg mouse models as well as human AD brain tissue will be necessary to fully determine the role of L-VSCCs in the pathophysiology of AD.

Acknowledgements

Work supported by NIH grants AG033649 to O.T.; AG004542 and AG010836 to P.W.L.; and AG027297 to C.M.N. The authors wish to thank Dr. Eric Blalock for important technical assistance.

References

[1] J.F. Disterhoft, J.R. Moyer Jr., L.T. Thompson, The calcium rationale in aging and Alzheimer's disease. Evidence from an animal model of normal aging, Ann. N. Y. Acad. Sci. 747 (1994) 382–406.
[2] T.C. Foster, C.M. Norris, Age-associated changes in Ca(2+)-dependent processes: relation to hippocampal synaptic plasticity, Hippocampus 7 (1997) 602–612.
[3] Z.S. Khachaturian, The role of calcium regulation in brain aging: reexamination of a hypothesis [published erratum appears in Aging (Milano) 1989;1(2):II], Aging (Milano) 1 (1989) 17–34.
[4] P.W. Landfield, T.A. Pitler, Prolonged Ca^{2+}-dependent afterhyperpolarizations in hippocampal neurons of aged rats, Science 226 (1984) 1089–1092.
[5] G.E. Stutzmann, The pathogenesis of Alzheimers disease is it a lifelong "calciumopathy"? Neuroscientist 13 (2007) 546–559.
[6] O. Thibault, J.C. Gant, P.W. Landfield, Expansion of the calcium hypothesis of brain aging and Alzheimer's disease: minding the store, Aging Cell 6 (2007) 307–317.
[7] I. Bezprozvanny, M.P. Mattson, Neuronal calcium mishandling and the pathogenesis of Alzheimer's disease, Trends Neurosci. 31 (2008) 454–463.
[8] O. Thibault, P.W. Landfield, Increase in single L-type calcium channels in hippocampal neurons during aging, Science 272 (1996) 1017–1020.
[9] M. Anantharaman, J. Tangpong, J.N. Keller, M.P. Murphy, W.R. Markesbery, K.K. Kiningham, D.K. St Clair, Beta-amyloid mediated nitration of manganese superoxide dismutase: implication for oxidative stress in a APPNLH/NLH X PS-1P264L/P264L double knock-in mouse model of Alzheimer's disease, Am. J. Pathol. 168 (2006) 1608–1618.
[10] R. Gray, R. Fisher, N. Spruston, D. Johnston, Preparations of the Vertebrate Central Nervous System In Vitro, Wiley, New York, 1990.
[11] C.M. Norris, E.M. Blalock, K.C. Chen, N.M. Porter, O. Thibault, S.D. Kraner, P.W. Landfield, Hippocampal 'zipper' slice studies reveal a necessary role for calcineurin in the increased activity of L-type Ca(2+) channels with aging, Neurobiol. Aging 31 (2010) 328–338.
[12] L.D. Brewer, A.L. Dowling, M.A. Curran-Rauhut, P.W. Landfield, N.M. Porter, E.M. Blalock, Estradiol reverses a calcium-related biomarker of brain aging in female rats, J. Neurosci. 29 (2009) 6058–6067.
[13] D.M. Mathis, J.L. Furman, C.M. Norris, Preparation of acute hippocampal slices from rats and transgenic mice for the study of synaptic alterations during aging and amyloid pathology, J. Vis. Exp. 49 (2011) e2330, doi:10.3791/2330.
[14] B. Sakmann, E. Neher, Patch clamp techniques for studying ionic channels in excitable membranes, Annu. Rev. Physiol. 46 (1984) 455–472.
[15] N.M. Porter, O. Thibault, V. Thibault, K.C. Chen, P.W. Landfield, Calcium channel density and hippocampal cell death with age in long-term culture, J. Neurosci. 17 (1997) 5629–5639.
[16] D.S. Olton, R.L. Isaacson, Hippocampal lesions and active avoidance, Physiol. Behav. 3 (1968) 719–724.
[17] C.M. Norris, S. Halpain, T.C. Foster, Reversal of age-related alterations in synaptic plasticity by blockade of L-type Ca^{2+} channels, J. Neurosci. 18 (1998) 3171–3179.
[18] O. Thibault, R. Hadley, P.W. Landfield, Elevated postsynaptic $[Ca^{2+}]$i and L-type calcium channel activity in aged hippocampal neurons: relationship to impaired synaptic plasticity, J. Neurosci. 21 (2001) 9744–9756.
[19] J.R. Moyer Jr., L.T. Thompson, J.P. Black, J.F. Disterhoft, Nimodipine increases excitability of rabbit CA1 pyramidal neurons in an age- and concentration-dependent manner, J. Neurophysiol. 68 (1992) 2100–2109.
[20] R.A. Deyo, K.T. Straube, J.F. Disterhoft, Nimodipine facilitates associative learning in aging rabbits, Science 243 (1989) 809–811.
[21] L.M. Veng, M.H. Mesches, M.D. Browning, Age-related working memory impairment is correlated with increases in the L-type calcium channel protein alpha1D (Cav1.3) in area CA1 of the hippocampus and both are ameliorated by chronic nimodipine treatment, Brain Res. Mol. Brain Res. 110 (2003) 193–202.
[22] A.L. Coon, D.R. Wallace, C.F. Mactutus, R.M. Booze, L-type calcium channels in the hippocampus and cerebellum of Alzheimer's disease brain tissue [In Process Citation], Neurobiol. Aging 20 (1999) 597–603.
[23] R.M. Davidson, L. Shajenko, T.S. Donta, Amyloid beta-peptide (A beta P) potentiates a nimodipine-sensitive L-type barium conductance in N1E-115 neuroblastoma cells, Brain Res. 643 (1994) 324–327.
[24] H. Fu, W. Li, Y. Lao, J. Luo, N.T. Lee, K.K. Kan, H.W. Tsang, K.W. Tsim, Y. Pang, Z. Li, D.C. Chang, M. Li, Y. Han, Bis(7)-tacrine attenuates beta amyloid-induced neuronal apoptosis by regulating L-type calcium channels, J. Neurochem. 98 (2006) 1400–1410.
[25] S. Kim, H. Rhim, Effects of amyloid-beta peptides on voltage-gated L-type Ca(V) 1.2 and Ca (V)1.3 Ca (2+) channels, Mol. Cells 32 (2011) 289–294.
[26] M. Ramsden, Z. Henderson, H.A. Pearson, Modulation of Ca^{2+} channel currents in primary cultures of rat cortical neurones by amyloid beta protein (1–40) is dependent on solubility status, Brain Res. 956 (2002) 254–261.
[27] J.L. Scragg, I.M. Fearon, J.P. Boyle, S.G. Ball, G. Varadi, C. Peers, Alzheimer's amyloid peptides mediate hypoxic up-regulation of L-type Ca^{2+} channels, FASEB J. 19 (2005) 150–152.
[28] K. Ueda, S. Shinohara, T. Yagami, K. Asakura, K. Kawasaki, Amyloid beta protein potentiates Ca^{2+} influx through L-type voltage-sensitive Ca^{2+} channels: a possible involvement of free radicals, J. Neurochem. 68 (1997) 265–271.
[29] N.J. Webster, M. Ramsden, J.P. Boyle, H.A. Pearson, C. Peers, Amyloid peptides mediate hypoxic increase of L-type Ca^{2+} channels in central neurones, Neurobiol. Aging 27 (2006) 439–445.
[30] J.H. Weiss, C.J. Pike, C.W. Cotman, Ca^{2+} channel blockers attenuate beta-amyloid peptide toxicity to cortical neurons in culture, J. Neurochem. 62 (1994) 372–375.
[31] M.A. Davare, J.W. Hell, Increased phosphorylation of the neuronal L-type Ca(2+) channel Ca(v)1.2 during aging, Proc. Natl. Acad. Sci. U. S. A. 100 (2003) 16018–16023.
[32] C.M. Norris, E.M. Blalock, K.C. Chen, N.M. Porter, P.W. Landfield, Calcineurin enhances L-type Ca(2+) channel activity in hippocampal neurons: increased effect with age in culture, Neuroscience 110 (2002) 213–225.
[33] D.L. Smith, J. Pozueta, B. Gong, O. Arancio, M. Shelanski, Reversal of long-term dendritic spine alterations in Alzheimer disease models, Proc. Natl. Acad. Sci. U. S. A. 106 (2009) 16877–16882.
[34] B. Gong, Z. Cao, P. Zheng, O.V. Vitolo, S. Liu, A. Staniszewski, D. Moolman, H. Zhang, M. Shelanski, O. Arancio, Ubiquitin hydrolase Uch-L1 rescues beta-amyloid-induced decreases in synaptic function and contextual memory, Cell 126 (2006) 775–788.
[35] K.T. Dineley, D. Hogan, W.R. Zhang, G. Taglialatela, Acute inhibition of calcineurin restores associative learning and memory in Tg2576 APP transgenic mice, Neurobiol. Learn. Mem. 88 (2007) 217–224.
[36] L.C. Reese, W. Zhang, K.T. Dineley, R. Kayed, G. Taglialatela, Selective induction of calcineurin activity and signaling by oligomeric amyloid beta, Aging Cell 7 (2008) 824–835.
[37] C.M. Norris, I. Kadish, E.M. Blalock, K.C. Chen, V. Thibault, N.M. Porter, P.W. Landfield, S.D. Kraner, Calcineurin triggers reactive/inflammatory processes in astrocytes and is upregulated in aging and Alzheimer's models, J. Neurosci. 25 (2005) 4649–4658.
[38] H.Y. Wu, E. Hudry, T. Hashimoto, K. Kuchibhotla, A. Rozkalne, Z. Fan, T. Spires-Jones, H. Xie, M. Arbel-Ornath, C.L. Grosskreutz, B.J. Bacskai, B.T. Hyman, Amyloid beta induces the morphological neurodegenerative triad of spine loss, dendritic simplification, and neuritic dystrophies through calcineurin activation, J. Neurosci. 30 (2010) 2636–2649.
[39] G.E. Stutzmann, I. Smith, A. Caccamo, S. Oddo, F.M. Laferla, I. Parker, Enhanced ryanodine receptor recruitment contributes to Ca^{2+} disruptions in young, adult, and aged Alzheimer's disease mice, J. Neurosci. 26 (2006) 5180–5189.
[40] P. Chavis, L. Fagni, J.B. Lansman, J. Bockaert, Functional coupling between ryanodine receptors and L-type calcium channels in neurons, Nature 382 (1996) 719–722.
[41] J.C. Gant, K.C. Chen, C.M. Norris, I. Kadish, O. Thibault, E.M. Blalock, N.M. Porter, P.W. Landfield, Disrupting function of FK506-binding protein 1b/12.6 induces the Ca(2)+-dysregulation aging phenotype in hippocampal neurons, J. Neurosci. 31 (2011) 1693–1703.
[42] J.C. Gant, M.M. Sama, P.W. Landfield, O. Thibault, Early and simultaneous emergence of multiple hippocampal biomarkers of aging is mediated by Ca^{2+}-induced Ca^{2+} release, J. Neurosci. 26 (2006) 3482–3490.
[43] A. Kumar, T.C. Foster, Enhanced long-term potentiation during aging is masked by processes involving intracellular calcium stores, J. Neurophysiol. 91 (2004) 2437–2444.
[44] G.E. Stutzmann, M.P. Mattson, Endoplasmic reticulum Ca(2+) handling in excitable cells in health and disease, Pharmacol. Rev. 63 (2011) 700–727.
[45] Y. Wang, N.H. Greig, Q.S. Yu, M.P. Mattson, Presenilin-1 mutation impairs cholinergic modulation of synaptic plasticity and suppresses NMDA currents in hippocampus slices, Neurobiol. Aging 30 (2009) 1061–1068.